European Radiology (2019) 29:4333–4340
https://doi.org/10.1007/s00330-018-5970-5

CHEST

Changes in quantitative parameters of pulmonary nonsolid nodule induced by lung inflation according to paired inspiratory and expiratory computed tomography imaging

Li Fan[1] · QingChu Li[1] · WenTing Tu[1] · RuTan Chen[1] · Yi Xia[1] · Yu Pu[1] · ZhaoBin Li[2] · ShiYuan Liu[1]

Received: 10 July 2018 / Revised: 7 November 2018 / Accepted: 13 December 2018 / Published online: 28 January 2019

Abstract

Objective To evaluate quantitative parameters of nonsolid nodules on paired inspiratory and expiratory computed tomography (CT) and to examine whether these parameters are sensitive to lung inflation reflected by lung volume.

Methods Thirty-three patients with 41 nonsolid nodules were included in this prospective study. Paired inspiratory and low-dose respiratory plain chest CT were performed. The volume and density of nonsolid nodule(s), both lungs, the right and left lung, and five lobes, were analyzed in inspiratory and expiratory CT scans. The ratio of expiratory to inspiratory parameters was calculated and labeled as parameter$_{(E-I)/I}$. To standardize the changes in nonsolid nodule quantitative parameters, the ratio of nonsolid nodule parameter to lung parameter was also calculated. Quantitative parameters were compared between inspiratory and expiratory CT.

Results Nonsolid nodule volumes on expiratory CT were reduced by 19.8% ± 12.9%, while the density was increased by 11.4% ± 8.8%. The volume of nonsolid nodules was significantly greater on inspiratory compared with expiratory CT ($p < 0.001$). The density of nonsolid nodules was significantly greater on expiratory than inspiratory CT ($p < 0.001$). The volume$_{(E-I)/I}$ was significantly greater than density$_{(E-I)/I}$ both in nonsolid nodules and lung. The volume$_{(E-I)/I}$ and density$_{(E-I)/I}$ of nonsolid nodules were independent of size. The density$_{(E-I)/I}$ of nonsolid nodule was greater in the lower lobe than that in the upper lobe ($p = 0.002$).

Conclusion Volume changes in nonsolid nodules were more sensitive than density changes in expiratory phase. The density of lower lobe nodules was more susceptible to respiration. Expiratory scanning is not recommended for quantification of nonsolid nodules and/or follow-up.

Key Points

- *The nonsolid nodule volume on expiratory CT was reduced by 19.8% ± 12.9%.*
- *The nonsolid nodule density on expiratory CT was increased by 11.4% ± 8.8%.*
- *The volume$_{(E-I)/I}$ and density$_{(E-I)/I}$ of nonsolid nodules were independent of size.*

Keywords Solitary pulmonary nodule · Tomography, x-ray computed · Computational biology

Li Fan and QingChu Li contributed equally to this work.

✉ ZhaoBin Li
lizhaobin79@163.com

✉ ShiYuan Liu
lsy0930@163.com

[1] Department of Radiology, Changzheng Hospital, Second Military Medical University, No. 415 Fengyang Road, Shanghai 200003, China

[2] Department of Radiation Oncology, Shanghai Jiao Tong University Affiliated Sixth People's Hospital, No. 600 Yishan Road, Shanghai 200233, China

Abbreviations

AEC	Automatic exposure control
CT	Computed tomography
IL	Ipsilateral lung
MLD	Mean lung density
Parameter$_{(E-I)/I}$	(Parameter$_{expiratory}$−Parameter$_{inspiratory}$)/ Parameter$_{inspiratory}$

Introduction

As more low-dose computed tomography (CT) lung cancer screening is performed worldwide, an increasing number of nonsolid nodules are detected. Pathologically, nonsolid nodule may be caused by partial airspace filling, interstitial thickening with inflammation, fibrosis, and neoplastic proliferation [1–3]. Nonsolid nodules are a non-specific finding on thin-section computed tomography; however, many early-stage lung adenocarcinomas manifest as nonsolid nodules on thin-section CT [4]. Most of the nonsolid nodule is inert; the follow-up CT is needed to evaluate changes. According to the Fleischner Society guideline for nonsolid nodules, size and density are the most important indices in the follow-up CT to determine persistence or increases in size or density, which would determine further management [5, 6]. In general, the measurement of volume and density is performed in apnea after full inspiration CT images are acquired. Moreover, the nature of malignant nonsolid nodules reflects a lepidic growth pattern, possibly susceptive to lung volume. Clinically, the scanning position changing would affect the shape or morphological features of nonsolid nodules, which may be caused by the degree of lung inflation [7]. Therefore, we hypothesized that the degree of lung inflation would affect the quantitative evaluation of the nonsolid nodules. This hypothesis is very important in the management of nonsolid nodules based on volume and density. To date, however, few studies focused on the effect of lung inflation on the quantitative assessment of nonsolid nodules. The purpose of this study was to quantitatively evaluate changes in nonsolid nodule parameters induced by the respiratory phase and to examine whether these parameters are sensitive to lung inflation, in an attempt to characterize physiological changes in different respiratory phases and inform more precise management of nonsolid nodules.

Materials and methods

Subject population

From December 2017 to March 2018, subjects who underwent routine non-contrast enhanced chest CT scanning and were admitted to the department of radiology in one hospital were enrolled in this prospective study. After routine chest CT scanning on end-inspiration, the images were evaluated by a 13-year experienced thoracic radiologist immediately and, if complying with all the following inclusion criteria, were included in this study. The inclusion criteria for nonsolid nodules were as follows: solitary or multiple lung nodule(s) manifesting as nonsolid nodule on thin-section (1 mm) inspiratory CT imaging, no solid or part-solid nodules, no calcified nodules, no emphysema (emphysema index < 6% [8]), and no other lung disease (e.g., COPD, any pattern of interstitial pneumonia and consolidation) affecting mean lung density (MLD). The MLD of normal pulmonary parenchyma on inspiratory CT is – 400 HU to – 899 HU [9]. Subjects with combined nodules, consisting of nonsolid and solid, or part solid, or calcified nodules were excluded. A total of 986 subjects underwent non-contrast enhanced chest CT scanning during this period. Among these subjects, 78 who exhibited solid/part-solid nodules, 113 who had calcified nodules, 176 with emphysema, 186 with fibrosing interstitial pneumonia, 28 with multiple lung nodules combining nonsolid nodule and solid, part solid, or calcified nodules, 68 with consolidation, and 304 with negative findings were excluded. The remaining 33 subjects (14 men, 19 women; age range, 30–77 years) with 41 nonsolid nodules were included in this study. The study was approved by the local ethics committee, and prospective written informed consent for study participation was obtained from all subjects after the nature of the procedure had been fully explained. All 33 included subjects underwent inspiratory and low-dose expiratory chest CT scanning. The two scans were performed with an interval of 3–5 min (time to read the inspiratory images).

CT scanning

All the subjects underwent imaging on a Philips Brilliance 256-slice CT (Philips Healthcare). Breath-hold training was performed before CT scanning. All the subjects were asked to hold apnea after full inspiration or expiration as long as possible. Non-contrast enhanced imaging was performed from the thoracic inlet to the middle portion of the kidneys. The following imaging parameters were used for inspiratory CT scanning: 120 kVp/dose modulation with automatic exposure control (AEC), slice thickness 1 mm, slice interval 1 mm, matrix of 512 × 512, collimation 128 × 0.625 mm, rotation 0.5 s, high-resolution algorithms, and iDose4 iterative reconstruction. To reduce exposure to radiation, the expiratory phase was performed at 120 kVp/50 mAs; other parameters were same as the inspiratory CT scanning, including the reconstruction algorithm.

Imaging analysis

Inspiratory and expiratory images were evaluated using lung density and lung nodule software on a post-processing workstation (Extended Brilliance Workspace TM, Philips Healthcare), respectively. Because lung density and volume are affected by lung inflation, to standardize changes in nonsolid nodule quantitative parameters, lung density and volume were investigated. The lung tissue was segmented semi-automatically at the lobe level, followed by fine adjustment of the fissure margin by manually verifying the coronal, sagittal, and axial plane slice by slice to ensure accurate segmentation of the lobe by a thoracic radiologist with 13 years of experience. The MLD and volume of both lungs, right lung, left lung, and five lobes were generated automatically and recorded. The nonsolid nodule was segmented semi-automatically; the nonsolid nodule margin was adjusted manually slice by slice on the three planes to ensure accurate

Table 1 Lung volume, lung density, nonsolid nodule volume and nonsolid nodule density on inspiratory and expiratory CT

Parameters	Inspiration	Expiration	p value
Both lung volume (cm^3)	4616.9 (1099.7)	2920.5 (1097.3)	< 0.001$^{\&}$
Right lung volume (cm^3)	2403.1 (561.0)	1592.2 (621.5)	< 0.001$^{\&}$
RUL volume (cm^3)	938.2 (198.1)	660.6 (242.5)	< 0.001$^{\&}$
RML volume (cm^3)	362.7 (113. 5)	305.8 (112.6)	< 0.001$^{\&}$
RLL volume (cm^3)	1150.4 (211.7)	693.3 (298.9)	< 0.001$^{\&}$
Left lung volume (cm^3)	2224.8 ± 445.5	1393.0 (512.3)	< 0.001$^{\&}$
LUL volume (cm^3)	1130.9 (200.8)	770.2 (311.6)	< 0.001$^{\&}$
LLL volume (cm^3)	1095.1 ± 243.7	657.9 (205.5)	< 0.001$^{\&}$
Both lung density (HU)	− 858 ± 25	− 792 ± 43	< 0.001
Right lung density (HU)	− 857 ± 25	− 798 (79)	< 0.001$^{\&}$
RUL density (HU)	− 865 ± 23	− 817 (73)	< 0.001$^{\&}$
RML density (HU)	− 869 (36)	− 831 ± 32	< 0.001$^{\&}$
RLL density (HU)	− 846 ± 30	− 755 ± 63	< 0.001
Left lung density (HU)	− 860 ± 25	− 794 ± 45	< 0.001
LUL density (HU)	− 869 ± 24	− 827 (64)	< 0.001$^{\&}$
LLL density (HU)	− 851 ± 29	− 773(68)	< 0.001$^{\&}$
Nonsolid nodule long axial (mm)	9 (7)	8 (6)	< 0.001$^{\&}$
Nonsolid nodule short axial (mm)	7 (4)	7 (5)	0.008$^{\&}$
Nonsolid nodule size (mm)	8 (5)	7 (5)	< 0.001$^{\&}$
Nonsolid nodule volume (cm^3)	0.3 (0.8)	0.2 (0.6)	< 0.001$^{\&}$
Nonsolid nodule density (HU)	− 659 ± 110	− 588 ± 128	< 0.001$^{\&}$

Data was expressed as mean ± standard deviation or median (interquartile range). $^{\&}$ Paired t test or Wilcoxon signed ranks test was used

segmentation by the same experienced thoracic radiologist. Both the lung and subsolid nodule segmentations were performed under another experienced (20 years) thoracic radiologist instruction. Consensus regarding the fine adjustment of margin of lung lobe and nonsolid nodule by the two experienced radiologists was reached. The segmentation reproducibility of intra- and inter-observer was confirmed in a previous study [10]. Long axis, short axis, volume, and mean density of nonsolid nodules were generated automatically and recorded. The size of nonsolid nodules was defined as the average of long axial and short axial [5]. Based on the clinical common threshold for lung nodule size evaluation and the T descriptor of 8th edition TNM stage of NSCLC [11, 12], nonsolid nodules were classified into two groups, < 10 mm and ≥ 10 mm. The changes in the abovementioned parameters, the ratio of expiratory parameter to inspiratory was calculated and defined as parameter$_{(E-I)/I}$ $\{(\text{Parameter}_{\text{expiratory}} - \text{Parameter}_{\text{inspiratory}})/\text{Parameter}_{\text{inspiratory}}\}$. To standardize changes in nonsolid nodule quantitative parameters more accurately, the ratio of nonsolid nodule volume to ipsilateral lung volume ($\text{Volume}_{\text{nonsolid nodule}}/\text{Volume}_{\text{IL}}$), ratio of nonsolid nodule volume to the corresponding lobe volume nonsolid nodule located ($\text{Volume}_{\text{nonsolid nodule}}/\text{Volume}_{\text{lobe}}$), ratio of nonsolid nodule density to ipsilateral lung density ($\text{Density}_{\text{nonsolid nodule}}/\text{Density}_{\text{IL}}$), and ratio of nonsolid nodule density to the corresponding lobe density nonsolid nodule located ($\text{Density}_{\text{nonsolid nodule}}/\text{Density}_{\text{lobe}}$) were also calculated, respectively.

Statistical analyses

Statistical analysis of all data sets was performed with SPSS 21.0 software (SPSS Inc). The normality of the distributions was tested using the Shapiro-Wilk test. The data are expressed in mean ± standard deviation or median (interquartile range). In terms of measurement data that were normally distributed, paired t test or independent sample T test was used; otherwise, statistics were analyzed using the Mann-Whitney U test or the Kruskal-Wallis test. A two-sided p value < 0.05 was considered to be statistically significant.

Results

There were 28 patients with solitary nonsolid nodules, four with two nonsolid nodules, and one with five nonsolid nodules. The size range of nonsolid nodules on the inspiratory phase was 6~23 mm with average size 10 mm ± 4 mm, and 6~21 mm with average size 10 mm ± 4 mm on the expiratory phase. Twenty-four nonsolid nodules were < 10 mm in mean size, 14 were between 10 mm and 20 mm, and three were > 20 mm on inspiratory CT imaging. Twelve ones were located in the right upper lobe, one in the right middle lobe, eight in the right lower lobe, 14 in the left upper lobe, and six in the left lower lobe.

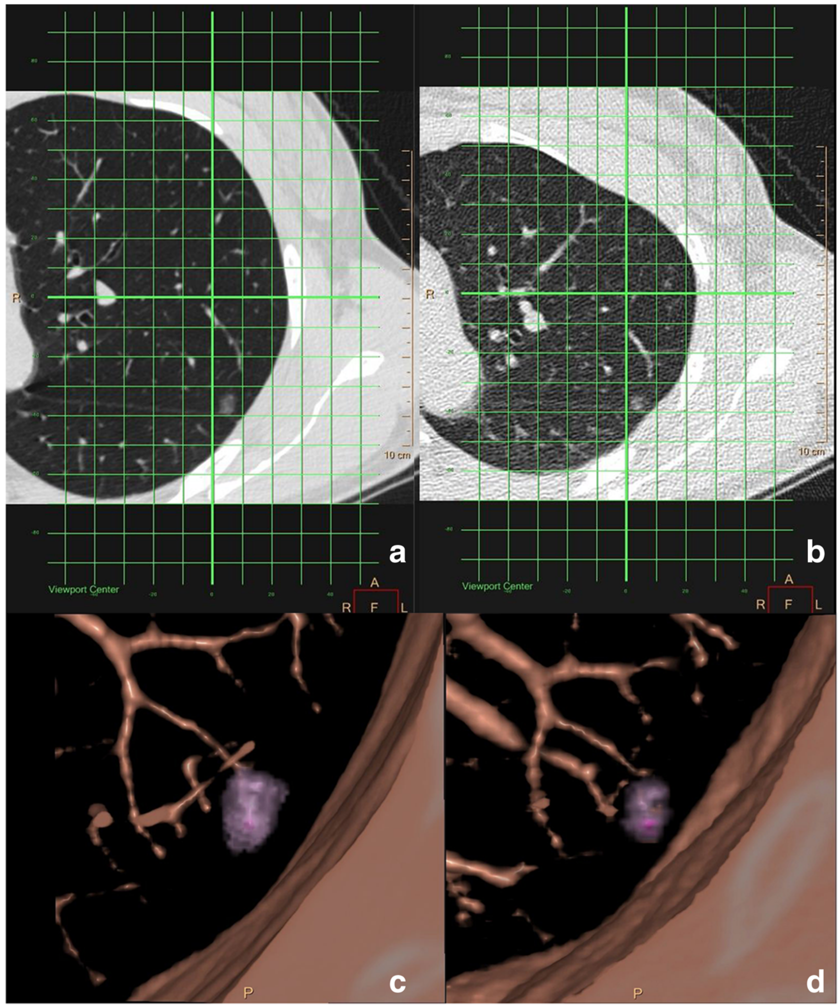

Fig. 1 Nonsolid nodule on paired inspiratory and expiratory phase CT axial images and volume rendering. A nonsolid nodule in the posterior segment of the left upper lobe, confirmed as minimally invasive adenocarcinoma by surgical pathology in a 35-year-old female. Inspiratory phase (**a**, **c**). Expiratory phase (**b**, **d**). The volume was 212 mm^3 and 184 mm^3 on inspiratory and expiratory CT, respectively. The mean density was − 698 HU and − 616 HU on inspiratory and expiratory CT, respectively

Lung volume and density at the lobe level on inspiratory and expiratory CT

The data presented in Table 1 revealed that all the lung volume parameters were significantly greater in the inspiratory phase than in the expiratory phase ($p < 0.001$). Lung density was significantly greater in the expiratory phase than in the inspiratory phase ($p < 0.001$).

Nonsolid nodule volume and density on inspiratory and expiratory CT

The long axial, short axial, size, and volume of nonsolid nodule on inspiratory CT was significantly greater than on expiratory CT images ($p < 0.001$, $p = 0.008$, $p < 0.001$, and $p < 0.001$, respectively) (Table 1). The mean density of nonsolid nodule on expiratory CT was greater than on inspiratory CT images (− 588 Hounsfield units [HU] ± 128 HU vs. – 659 HU ± 110 HU, $p < 0.001$) (Figs. 1 and 2).

Comparison of quantitative parameter ratio on inspiratory and expiratory CT

To standardize changes in quantitative parameters of nonsolid nodule, the ratio of each parameter to the ipsilateral lung and the located lobe was calculated and compared (Table 2). Neither the $Volume_{nonsolid\ nodule}/Volume_{IL}$ nor the $Volume_{nonsolid\ nodule}/Volume_{lobe}$ was statistically different between inspiratory and expiratory CT ($p = 0.418$, $p = 0.058$, respectively). Both $Density_{nonsolid\ nodule}/Density_{IL}$ and $Density_{nonsolid\ nodule}/Density_{lobe}$ were significantly greater on inspiratory CT than on expiratory CT ($p = 0.025$, $p = 0.004$, respectively).

The quantitative parameters of change ratio on expiratory CT relative to those on inspiratory CT are listed in Table 3. The $volume_{(E-I)/I}$ was significantly greater than the $density_{(E-I)/I}$, not only in nonsolid nodule but also in the lung and the ratio of nonsolid nodule to lung parameters. Nonsolid nodule size and volume on expiratory CT was reduced by 6.9% ± 7.8% and 19.8% ± 12.9%, respectively, while the density was increased by 11.4% ± 8.8% (Fig. 2).

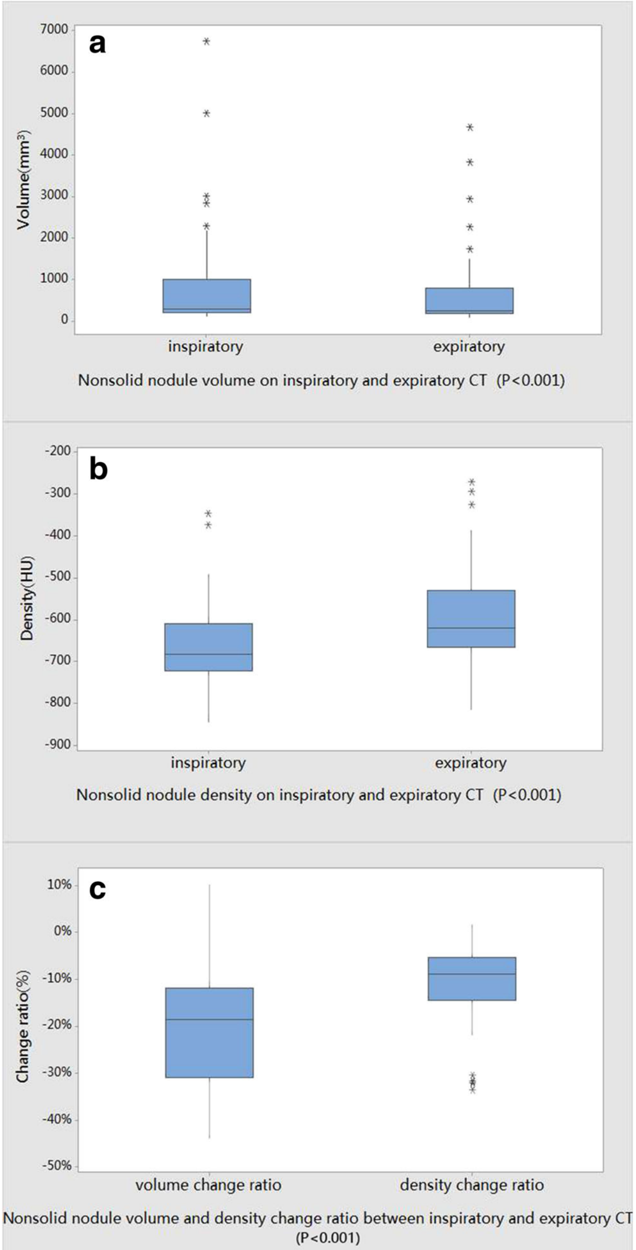

Fig. 2 Boxplot of pulmonary nonsolid nodule volume, density, and change ratio on inspiratory and expiratory CT. Volume (**a**), density (**b**), volume change ratio and density change ratio (**c**). Volume change ratio = $volume_{(E-I)/I}$, Density change ratio = $density_{(E-I)/I}$

Comparison of quantitative parameter ratio between different size and different lobe of nonsolid nodules

The quantitative parameters of change ratio on expiratory CT relative to inspiratory CT were also compared among different sizes of nonsolid nodule. Due to the small sample size of nonsolid nodule > 20 mm ($n = 3$), it was merged with nonsolid nodule between 10 and 20 mm into one group. The nonsolid nodules were classified into two groups, < 10 mm and ≥ 10 mm.

Table 2 Volume and density ratio of nonsolid nodule to ipsilateral lung and lobe on inspiratory and expiratory CT

Parameters (%)	Inspiration	Expiration	*p* value
$Volume_{nonsolid\ nodule}/Volume_{IL}$	0.01 (0.04)	0.01 (0.04)	0.418#
$Volume_{nonsolid\ nodule}/Volume_{lobe}$	0.03 (0.08)	0.04 (0.08)	0.058#
$Density_{nonsolid\ nodule}/Density_{IL}$	79.2 (13.5)	77.1 (17.4)	0.025#
$Density_{nonsolid\ nodule}/Density_{lobe}$	76.3 ± 11.7	73.5 ± 15.0	0.004*

Data was expressed as mean ± standard deviation or median (interquartile range). *IL*, ipsilateral lung; *lobe*, the lobe that nonsolid nodule was located. # Wilcoxon signed ranks test. *Paired *t* test

No difference was found in nonsolid nodule $volume_{(E-I)/I}$ and $density_{(E-I)/I}$ between the two groups ($p = 0.352$, $p = 0.195$, respectively) (Table 4), while in the same group, the nonsolid nodule $volume_{(E-I)/I}$ was greater than $density_{(E-I)/I}$ ($p = 0.009$, $p = 0.044$, respectively).

The quantitative parameters of change ratio on expiratory CT relative to inspiratory CT were also compared in different lobe of nonsolid nodule. The nonsolid nodule in right middle lobe ($n = 1$) was excluded for this analysis. The $density_{(E-I)/I}$ of nonsolid nodule was significantly greater in the lower lobe than that in the upper lobe ($p = 0.002$) (Table 5). No difference was found in volumetric parameter between the upper and lower lobes ($p = 0.066$).

Discussion

Significant differences were found in volume and density of nonsolid nodules between the inspiratory and expiratory phases on CT imaging. Moreover, changes in volume and density of nonsolid nodule were independent of size. The changes in nonsolid nodule density were associated with location, and the lower lobe nodules were more susceptible to variation in respiration (Table 5). Our study provided novel insights on the quantification of nonsolid nodule and the degree of lung inflation without any comparative studies in the literature. This was the first study to evaluate changes in the volume and density of nonsolid nodules on paired inspiratory and expiratory CT.

Due to the negative pressure of the thoracic cage during inspiration, more air is inhaled to inflate the lung. In the present study, both the volume of the entire lung and each lobe decreased from end-inspiration to end-expiration, which has been reported in some studies, not only with CT but also with magnetic resonance imaging (MRI) [13, 14]. Unilateral lung volume was reduced in the expiratory phase. A previous study investigating the effect of lung inflation on pulmonary perfusion using MRI in health volunteers reported that the area was larger on end-inspiration than on end-expiration [14]. Lung density in vivo on CT is the combination of the pulmonary

Table 3 Quantitative parameters of change ratio on expiratory CT relative to inspiratory CT

Parameter (E-I)/I	Range (%)	Mean ± SD/median (IQR) (%)	p value
Nonsolid nodule parameters			
Nonsolid nodule long axial	(− 28.9~5.6)	− 8.0 ± 6.6	< 0.001
Nonsolid nodule short axial	(− 34.2~25.7)	− 5.2 ± 13.2	
Nonsolid nodule size	(− 24.7~8.7)	− 6.9 ± 7.8	
Nonsolid nodule volume	(− 43.9~10.4)	− 19.8 ± 12.9[a]	
Nonsolid nodule density	(− 33.5~1.8)	− 11.4 ± 8.8[a]	
Lung parameters			
IL volume	(− 49.7~7.2)	− 27.5 (28.9)[b]	0.001
IL density	(− 15.6~0.4)	− 7.7 ± 4.1[b]	
Lobe volume	(− 50.6~66.5)	− 30.2 (26.2)[c]	
Lobe density	(− 17.5~0.6)	− 7.4 ± 4.7[c]	
Ratio of nonsolid nodule to lung parameters			
$Volume_{nonsolid\ nodule}/Volume_{IL}$	(− 43.9~87.5)	0.8 (34.1)	< 0.001
$Volume_{nonsolid\ nodule}/Volume_{lobe}$	(− 49.8~81.4)	14.0 ± 27.0 [d]	
$Density_{nonsolid\ nodule}/Density_{IL}$	(− 24.5~14.1)	− 1.5 (7.3)	
$Density_{nonsolid\ nodule}$/Densitylobe	(− 22.4~9.1)	− 2.0 (7.8)[d]	

IQR, interquartile range; *Parameter (E-I)/I*, ($Parameter_{expiratory}$−$Parameter_{inspiratory}$)/$Parameter_{inspiratory}$; *IL*, ipsilateral lung; *lobe*, the lobe that nonsolid nodule was located. The Kruskal-Wallis test was performed in nonsolid nodule parameters, lung parameters, and the ratio of nonsolid nodule to the lung parameters. [a] Significant difference was found (statistic value 10.81, $p = 0.001$). [b] Significant difference was found (statistic value 17.46, $p < 0.001$). [c] Significant difference was found (statistic value 29.89, $p < 0.001$). [d] Significant difference was found (statistic value 13.32, $p < 0.001$)

parenchyma, interstitial, and blood. It has been confirmed that blood plays a significant role in lung density/weight in pig. Compared with bloodless conditions in pigs, CT obtained in vivo consistently overestimated lung weight/density because it included pulmonary blood [15]. Lung density reflects the pulmonary interstitial structure, especially the bronchovascular bundle. The increase in vascular density is proportional to a decrease in lung volume. It is known that lung inflation has a significant effect on the pressure-flow relationship of the pulmonary vasculature. Lung inflation affects the pulmonary vasculature by compressing the small pulmonary vessels, which leads to a significant amount of blood expelled from the pulmonary circulatory system [16]. Accordingly, pulmonary blood flow is less in a high state of lung inflation than in a low state (i.e., inspiration vs. expiration) at the same cardiac phase. This would cause a decrease in MLD. Meanwhile, more air in the alveolar would further decrease MLD. In this study, higher density was observed on end-expiration than on end-inspiration, which corresponds to the normal physiological process. Unilateral lung density was increased in the expiratory phase.

In the guidelines for the management of incidental pulmonary nodules detected on CT images [5, 17], the size is one of the most important indices used to determine management strategy. For nonsolid nodules that require further follow-up CT scanning, size assessment is essential. In this study, the size of nonsolid nodules changed significantly between the different respiratory phases. Table 1 shows that size and volume were significantly reduced in the expiratory phase. Nonsolid nodule volume declined with the reduction in lung volume in expiratory phase, indicating that the nature of nonsolid nodule is not completely solid and is vulnerable to lung inflation, which may be related to its pathological basis, with most manifesting in a lepidic growth pattern along the

Table 4 Quantitative parameters of change ratio on expiratory CT relative to inspiratory CT in different size of nonsolid nodules

Parameters	< 10 mm ($n = 24$)	≥ 10 mm ($n = 17$)	p value
Mean size	7 mm ± 1 mm	13 mm (6 mm)	< 0.001[&]
Nonsolid nodule $volume_{(E-I)/I}$	− 18.2% ± 13. 9%[#]	− 22.0% ± 11.3%[$]	0.352*
Nonsolid nodule $density_{(E-I)/I}$	− 8. 6% (7.7%)[#]	− 14.2% ± 10.7%[$]	0.195[&]

Data was expressed as mean ± standard deviation or median (interquartile range). [#] Significant difference was found with Mann-Whitney *U* test (statistic value − 2.598, $p = 0.009$); [$] Significant difference with independent samples *t* test (statistic value − 2.095, $p = 0.044$). [&] Mann-Whitney *U* test. *Independent samples *t* test

Table 5 Quantitative parameters of change ratio on expiratory CT relative to inspiratory CT in the upper lobe and lower lobes

Parameter (E-I)/I	Upper lobe ($n = 26$) (%)	Lower lobe ($n = 14$) (%)	p value
Nonsolid nodule volume	− 17.2 ± 12.5	− 25.1 ± 12.6	0.066*
Nonsolid nodule density	−7.8 ± 4.4	− 18.6 ± 10.7	0.002*
Nonsolid nodule long axial	− 6.7 ± 6.0	− 10.8 ± 7.2	0.063*
Nonsolid nodule short axial	− 6.6 ± 12.1	− 2.1 ± 15.3	0.319*
Nonsolid nodule size	− 6.8 ± 7.5	− 7.3 ± 9.0	0.864*
Lobe density	− 6.1 ± 3.3	− 10.1 ± 5.9	0.031*
Lobe volume	− 26.5 ± 13.8	− 40.4 (22.5)	0.065&
$Volume_{nonsolid\ nodule}/Volume_{lobe}$	15.8 ± 24.5	12.1 ± 32.5	0.684*
$Density_{nonsolid\ nodule}/Density_{lobe}$	− 1.7 ± 4.8	− 10.3 (22.6)	0.094&

Data was expressed as mean ± standard deviation or median (interquartile range)

*Independent samples t test. & Mann-Whitney U test

Parameter (E-I)/I, $(Parameter_{expiratory}-Parameter_{inspiratory})/Parameter_{inspiratory}$; *IL*, ipsilateral lung; *lobe*, the lobe that subsolid nodule was located

alveolar. Volume doubling time plays an important role in the differential diagnosis of nonsolid nodule; therefore, volume quantification should be accurate, and any change caused by physiological factors should be excluded. Therefore, during the follow-up CT scanning, the degree of lung inflation plays a major role in accurately determining changes in nonsolid nodules. In this study, only two points, end-inspiration and end-expiration, were assessed, and the degree of lung inflation may be different among patients due to lack of the quantitative assessment of lung inflation, which in turn may have affected the results. Ideally, a 4D respiratory gating CT technique may be recommended in nonsolid nodule quantification follow-up to ensure the same lung inflation degree at any time point in the respiratory cycle. However, in the clinic, a more practical suggestion would be the mandatory use of thin section (1 mm), which would enable optimal comparison of anatomical landmarks between scans to ensure the degree of respiratory effort to be as consistent as possible, which is especially important when using cross-sectional measurements. Furthermore, whenever possible, follow-up studies should be performed using the same equipment with the same software when available.

Nonsolid nodule density is another important parameter with regard to differential diagnosis, predicting growth, identifying pathological invasiveness of lung adenocarcinomas, and prognosis [18–20]. It has been reported that nonsolid nodule with a maximum diameter of ≤ 10 mm and a CT value ≤ − 600 HU is nearly always preinvasive lesions [21]. Therefore, accurate quantification of nonsolid nodule density is very important. Lung density changes in the paired inspiratory and expiratory phase have been widely explored in COPD, evaluating the E/I MLD and air trapping [9, 22]. No studies reported in the literature focused on density changes in nonsolid nodules in different respiratory phases. In this study, we found that nonsolid nodule density was increased by 11.4% ± 8.8% in expiratory phase compared with the inspiratory phase. The increase in nonsolid nodule density is proportional to a decrease in nonsolid nodule volume, which is similar to changes in the lung. Moreover, the changes in density in nonsolid nodules of the lower lobe were significantly greater than in the upper lobe; thus, supporting the speculation of which may be more affected by respiration status. The respiratory state (i.e., the degree of lung inflation) affects the volume and density of nonsolid nodules. Therefore, the degree of lung inflation should be considered in the quantitative analysis of nonsolid nodules to avoid misinterpretation of the results.

To standardize changes in parameters in different respiratory phases, the ratio of nonsolid nodule parameters to lung parameters were calculated and compared. Table 3 shows that $Volume_{nonsolid\ nodule}/Volume_{lobe}$ was greater than $Density_{nonsolid\ nodule}/Density_{lobe}$. The volume change in nonsolid nodules was greater than the density change, same as the lung parameters, indicating the volume is more sensitive to lung inflation than density. When evaluating volume, more attention should be devoted to the degree of lung inflation. Management of nonsolid nodules depends on nodule size. According to the 2017 Fleischner Society guideline, the threshold size is 6 mm (100 mm^3). The size range of nonsolid nodules in this study was 6~23 mm in the inspiratory phase, and 10 mm was set as the threshold to evaluate the difference in $volume_{(E-I)/I}$ and $density_{(E-I)/I}$ between different sizes of nonsolid nodules. We found that the $volume_{(E-I)/I}$ and $density_{(E-I)/I}$ of nonsolid nodules were independent of size. This is consistent with the threshold of Fleischner Society guideline, regardless of whether its size > 10 mm; therefore, only one size threshold 6 mm is essential. To reduce radiation exposure, expiratory CT was performed using low-dose CT (120 KV/50 mAs) and iDose4 iterative reconstruction. Previous studies have reported the effect of dose reduction on the quantification of phantom and lung nodule, including density, volume, and texture features [23–25]. However, iDose4 iterative reconstruction was used in this study, which could help to reduce the effect on the quantification of lung nodules.

This study has some limitations; the first of which was its prospective design and relatively small sample size. Second, the quantitative parameters of nonsolid nodule were derived from the results of semiautomatic segmentation; however, consensus on segmentation was reached by two experienced thoracic radiologists and validated in a previous study [10]. Third, small internal vessels and bronchi could not be excluded, which may have affected the attenuation of the subsolid nodule. Fourth, the low-dose CT scanning in the expiratory phase may affect the quantification of nonsolid nodules, which was not taken into account in this study. In future studies, more nonsolid nodules should be included in further research to obtain more accurate results for changes in quantitative parameters at different respiratory phases.

In conclusion, the degree of lung inflation could affect the volume and density of nonsolid nodules, and changes in volume were more sensitive than changes in density in the expiratory phase. Expiratory scanning is not recommended for quantification of nonsolid nodules and/or follow-up. Moreover, inspiratory scanning should ensure lung inflation as consistent as possible in follow-up CT to inform more precise management of nonsolid nodules.

Funding This study has received funding by the National Key R&D Program of China (grant numbers 2016YFE0103000 and 2017YFC1308703), the National Natural Science Foundation of China (grant Numbers 81871321 and 81370035), and the Youth Fund of the National Natural Science Foundation of China (grant number 81501618).

Compliance with ethical standards

Guarantor The scientific guarantor of this publication is Prof. ShiYuan Liu.

Conflict of interest The authors of this manuscript declare no relationships with any companies, whose products or services may be related to the subject matter of the article.

Statistics and biometry One of the authors has significant statistical expertise.

Informed consent Written informed consent was obtained from all subjects (patients) in this study.

Ethical approval Institutional Review Board approval was obtained.

Methodology
- prospective
- experimental
- performed at one institution

Publisher's note Springer Nature remains neutral with regard to jurisdictional claims in published maps and institutional affiliations.

References

1. Kim HY, Shim YM, Lee KS, Han J, Yi CA, Kim YK (2007) Persistent pulmonary nodular ground-glass opacity at thin-section CT: histopathologic comparisons. Radiology 245:267–275
2. Nakajima R, Yokose T, Kakinuma R, Nagai K, Nishiwaki Y, Ochiai A (2002) Localized pure ground-glass opacity on high resolution CT: histologic characteristics. J Comput Assist Tomogr 26:323–329
3. Yanagawa M, Johkoh T, Noguchi M et al (2017) Radiological prediction of tumor invasiveness of lung adenocarcinoma on thin-section CT. Medicine (Baltimore) 96:e6331
4. Goo JM, Park CM, Lee HJ (2011) Ground-glass nodules on chest CT as imaging biomarkers in the management of lung adenocarcinoma. AJR Am J Roentgenol 196:533–543
5. MacMahon H, Naidich DP, Goo JM et al (2017) Guidelines for management of incidental pulmonary nodules detected on CT images: from the Fleischner Society 2017. Radiology 284:228–243
6. Naidich DP, Bankier AA, MacMahon H et al (2013) Recommendations for the management of nonsolid pulmonary nodules detected at CT: a statement from the Fleischner Society. Radiology 266:304–317
7. Wang Y, Fan L, Liu SY, Li Q, Chen R (2016) Diagnostic value of CT target scanning combining with changing position for pulmonary nodule in special location. Journal of Practical Radiology 32:694–698
8. Lynch DA, Austin JH, Hogg JC et al (2015) CT-definable subtypes of chronic obstructive pulmonary disease: a statement of the Fleischner Society. Radiology 277:192–205
9. Kim EY, Seo JB, Lee HJ et al (2015) Detailed analysis of the density change on chest CT of COPD using non-rigid registration of inspiration/expiration CT scans. Eur Radiol 25:541–549
10. Fan L, Fang M, Li Z et al (2018) Radiomics signature: a biomarker for the preoperative discrimination of lung invasive adenocarcinoma manifesting as a ground-glass nodule. Eur Radiol. https://doi.org/10.1007/s00330-018-5530-z
11. Kishi K, Homma S, Kurosaki A et al (2004) Small lung tumors with the size of 1cm or less in diameter: clinical, radiological, and histopathological characteristics. Lung Cancer 44:43–51
12. Rami-Porta R, Bolejack V, Crowley J et al (2015) The IASLC lung cancer staging project: proposals for the revisions of the T descriptors in the forthcoming eighth edition of the TNM classification for lung cancer. J Thorac Oncol 10:990–1003
13. Yamashiro T, Matsuoka S, Bartholmai BJ et al (2010) Collapsibility of lung volume by paired inspiratory and expiratory CT scans: correlations with lung function and mean lung density. Acad Radiol 17:489–495
14. Fan L, Liu SY, Xiao XS, Sun F (2010) Demonstration of pulmonary perfusion heterogeneity induced by gravity and lung inflation using arterial spin labeling. Eur J Radiol 73:249–254
15. Protti A, Iapichino GE, Milesi M et al (2014) Validation of computed tomography for measuring lung weight. Intensive Care Med Exp 2:31
16. West JB (2012) Respiratory physiology—the essentials, 9th edn. Lippincott Williams and Wilkins, Baltimore
17. Alpert JB, Ko JP (2018) Management of incidental lung nodules: current strategy and rationale. Radiol Clin North Am 56:339–351
18. Yu WS, Hong SR, Lee JG et al (2016) Three-dimensional ground glass opacity ratio in C T images can predict tumor invasiveness of stage Ia lung cancer. Yonsei Med J 57:1131–1138
19. Sakakura N, Inaba Y, Yatabe Y et al (2016) Estimation of the pathological invasive size of pulmonary adenocarcinoma using high-resolution computed tomography of the chest: a consideration based on lung and mediastinal window settings. Lung Cancer 95:51–56
20. Son JY, Lee HY, Kim JH et al (2016) Quantitative CT analysis of pulmonary ground-glass opacity nodules for distinguishing invasive adenocarcinoma from non–invasive or minimally invasive adenocarcinoma: the added value of using iodine mapping. Eur Radiol 26:43–54
21. Kitami A, Sano F, Hayashi S et al (2016) Correlation between histological invasiveness and the computed tomography value in pure ground-glass nodules. Surg Today 46:593–598
22. Hersh CP, Washko GR, Estépar RS et al (2013) Paired inspiratory-expiratory chest CT scans to assess for small airways disease in COPD. Respir Res 14:42
23. Lo P, Young S, Kim HJ, Brown MS, McNitt-Gray MF (2016) Variability in CT lung-nodule quantification: effects of dose reduction and reconstruction methods on density and texture-based features. Med Phys 43:4854–4865
24. Doo KW, Kang EY, Yong HS, Woo OH, Lee KY, Oh YW (2014) Accuracy of lung nodule volumetry in low-dose CT with iterative reconstruction: an anthropomorphic thoracic phantom study. Br J Radiol 87:20130644
25. Maruyama S, Fukushima Y, Miyamae Y, Koizumi K (2018) Usefulness of model-based iterative reconstruction in semi-automatic volumetry for ground-glass nodules at ultra-low-dose CT: a phantom study. Radiol Phys Technol 11:235–241